



OPEN

Continuous decline of climate fluctuations in the Kunlun–Pamir Plateau from the perspective of the bioclimatic variables

Xiaoran Huang^{1,2,3,4}, Anming Bao^{1,5,6✉}, Yanfeng Wu⁷, Guoxiong Zheng^{8,9}, Tao Yu^{1,2,4}, Ye Yuan¹, Tao Li^{1,3,4}, Ting Wang^{1,3,4}, Lei Zheng¹⁰, Liangliang Jiang¹¹, Jiayu Bao¹², Vincent Nzabarinda¹, Philippe De Maeyer^{4,5} & Tim Van de Voorde^{4,5}

Understanding the changes in bioclimatic indicators is a prerequisite and foundation for biodiversity simulation and prediction of climate sensitive organisms. However, in high-altitude areas that are extremely sensitive to climate change, the long-term evolution patterns of bioclimatic indicators are still limited in understanding. For this purpose, we selected the Kunlun–Pamir Plateau, an irreplaceable biodiversity hotspot, as the research area, and to analyze the spatiotemporal evolution characteristics of bioclimatic indicators. We employed trend analysis, Empirical Orthogonal Function (EOF), and continuous wavelet analysis to conduct spatiotemporal analysis on 19 bioclimate indicators. We found that (1) Temporally, Mean Diurnal Range, Isothermality, Temperature Seasonality, Temperature Annual Range, Precipitation Seasonality are all trending downward in the time series; Spatially, the trend of change shows spatial variability. Central Kunlun is experiencing the biggest increases in energy factors. A western part of the Kunlun Pamir Plateau exhibits the pronounced rises in water factors. (2) The first two EOFs of 15 bioclimatic variables explained over 50% of the total variance, showing significant variations and spatial heterogeneity. (3) Regarding the periodicity: bioclimatic variables showed no significant periodicity, with the majority of events occurring at irregular intervals of 1–4 years and in different years. These insights enhance our understanding of climate characteristics in the Kunlun–Pamir Plateau, providing valuable input for devising effective biodiversity conservation strategies.

Keywords Climate fluctuations, Bioclimatic variables, Empirical orthogonal function, Wavelet power spectrum, Kunlun–Pamir Plateau

Climate change presents humanity with unprecedented challenges, particularly in high-altitude regions sensitive to climate variability^{1,2}. Bioclimatic indicators provide a comprehensive insight into how various species respond to climatic conditions. Therefore, bioclimatic variables not only reflect the characteristics of climate change, but also have biological significance^{3,4}. Understanding changes in bioclimatic indicators is essential for uncovering the physiological and ecological mechanisms driving species distribution⁵. The Research on bioclimatic variables

¹Key Laboratory of Ecological Safety and Sustainable Development in Arid Lands, Xinjiang Institute of Ecology and Geography, Chinese Academy of Sciences, Ürümqi 830011, China. ²Xinjiang Common University Key Lab of Smart City and Environmental Stimulation, College of Resource and Environmental Sciences, Xinjiang University, Ürümqi 830046, China. ³University of Chinese Academy of Sciences, Beijing 100049, China. ⁴Department of Geography, Ghent University, 9000 Ghent, Belgium. ⁵Sino-Belgian Joint Laboratory of Geo-Information, Ürümqi 830011, China. ⁶China-Pakistan Joint Research Center on Earth Sciences, CAS-HEC, Islamabad 45320, Pakistan. ⁷Northeast Institute of Geography and Agroecology, Chinese Academy of Sciences, Changchun 130102, Jilin, China. ⁸College of Earth and Environmental Sciences, Lanzhou University, Lanzhou 730000, China. ⁹Midui Glacier-Guangxie Lake Disaster Field Science Observation and Research Station of Tibet Autonomous Region, Northwest Institute of Eco-Environment and Resources, Chinese Academy of Sciences, Lanzhou 730000, China. ¹⁰State Key Laboratory of Soil Erosion and Dryland Farming On the Loess Plateau, Institute of Soil and Water Conservation, Northwest A&F University, Yangling 712100, China. ¹¹School of Geography and Tourism, Chongqing Normal University, Chongqing 401331, China. ¹²Kunming University of Science and Technology, Kunming 650093, Yunnan Province, China. [✉]email: baoam@ms.xjb.ac.cn

contributes to the development of environmental policies and sustainable management as well as to climate change mitigation efforts.

Bioclimatic indicator research has experienced significant progress in recent years, as evidenced by advances in data acquisition, technological advancements, methodological approaches, and the development of meaningful conclusions⁶. There are currently 40 indicators for bioclimatic variables, among which BIO1 to BIO11 are temperature-based. BIO12 to BIO19 are based on precipitation⁷. BIO20 to BIO27 are based on solar radiation, BIO28 to BIO35 are based on soil moisture⁸. Bio36 to Bio40 represent the first five principal components of the first 35 Bioclim variables in the CliMond 1975H dataset⁹. Due to the ease of obtaining temperature and precipitation data, most global datasets include the first 19 bioclimatic variables⁹. The commonly used bioclimatic variable datasets are WorldClim¹⁰, CHELSA¹¹, MERRAclim¹², and CMCC-BioClimInd⁶. These datasets are global-scale datasets with various spatial resolutions⁶ and have been widely used in Species Distribution Models (SDMs)¹³. However, these datasets encounter problems related to discontinuous time series and uncertain accuracy in high-altitude areas, particularly in mountainous regions¹⁴. The BIO1-BIO19 variables were selected for analysis due to their coverage of essential aspects of temperature and precipitation, which are crucial for understanding the climate dynamics of a region. These variables offer a comprehensive representation of climatic conditions and their variations¹⁵. Furthermore, their widespread use in ecological and climate studies ensures that our analysis adheres to established scientific methodologies, facilitating comparisons with other research.

Despite these advances, there remains a critical gap in the exploration of bioclimatic indicators for high-altitude regions, which are highly sensitive to the process of global warming. Due to the limited number of comprehensive studies in these elevated ecosystems, a complete understanding of their intricate ecological dynamics is lacking. Located at an average elevation of over 3900 m above sea level, the Kunlun–Pamir Plateau is a geographically unique and environmentally valuable region far from densely populated human areas¹⁶. The changes in the ecological environment of this region are mainly influenced by climate change. Previous studies on climate change in the Kunlun Pamir region have mostly focused on changes in glacier area, glacier mass, and snow cover. Research indicates an increasing trend in snow water equivalent in the Kunlun Pamir region¹⁷, while the eastern Pamir region experiences glacier retreat due to rising temperatures¹⁸. Glaciers in the western Kunlun Mountains exhibit a balanced or slightly positive mass balance¹⁹. However, direct climate-related studies are scarce. Compared to conventional climate change studies, investigating climate change from the perspective of bioclimatic variables allows for a more comprehensive examination, capturing a broader spectrum of climate changes. Bioclimatic variables is that they directly reflect the impact of climate on biological processes and ecosystems, support ecological models and future climate predictions, quantify the ecological effects of climate change, and are suitable for both global and regional scale studies. CRU provides global gridded data with a higher spatial resolution, which allows for better representation of the entire Kunlun–Pamir Plateau. Additionally, CRU data has long-term consistency and includes a wide range of climatic variables, making it more suitable for analyzing the broader and more complex climate trends of the plateau^{20,21}.

The purpose of this study is to analyze the spatial and temporal changes in Kunlun–Pamir Plateau and also further investigated their periodic variations basing 19 bioclimatic variables. This contributes to providing recommendations and support for the environmental and ecological protection of the Kunlun–Pamir region.

Data and methods

Study area

The Kunlun–Pamir Plateau is mainly located in China, with extensions into Pakistan, India, Afghanistan, Tajikistan, and Kyrgyzstan. The Kunlun–Pamir Plateau is subdivided into the sub-regions of Pamir, Karakoram, West KunLun, and East KunLun (Fig. 1). The altitude of the mountains ranges from 696 to 7356 m, with an average elevation of 3900 m. The mountains span over 2760 km from east to west and around 130–436 km from north to south. The terrain is characterized by steep slopes and towering peaks. The study region is greatly influenced by the predominant westerly winds. Moreover, and distinguished by extensive coverage of modern glaciers, resulting its unique ecological characteristics^{22,23}. At 5000 m altitude, annual precipitation can reach 200 mm, and at 5900 m altitude, 400 mm¹⁶. The dominant vegetation types in the region are alpine meadows and alpine steppes, with a few pockets of alpine scrub and coniferous forests^{24,25}. The Kunlun–Pamir Plateau is rich in biodiversity and provides habitat for wildlife species. Among them, notable species include Siberian ibex, Kiang, wild yak, Ovis ammon, Tibetan antelope, snow leopard, brown bear, etc^{26–28}.

Bioclimatic variables

This study is based on global gridded observational data provided by the CRU at the University of East Anglia, UK (<http://www.cgiar-csi.org/>), with a spatial resolution of 0.5°. It spans from 1850 to the present with monthly resolution. The CRU was selected to generate the 19 bioclimate variables because its trends in annual, spring, summer, and autumn precipitation have been shown to be consistent with observed values on the Tibetan Plateau^{20,29} and has been extensively applied in climate change studies situated in high-altitude areas^{30–32}. We selected monthly precipitation, minimum temperature, and maximum temperature data from CRU. The 19 bioclimatic variables listed in Table 1 were calculated using the function “biocv” from the R package “dismo”, in accordance with the calculation method employed in WorldClim for bioclimatic variables. A quarter refers to a period of 3 months (1/4 of the year).

Analytical methods

This study comprehensively examines trends, principal modes, spatial structures, and periodic characteristics of the 19 bioclimatic variables at different time intervals, integrating multiple analytical methods. To simplify the data and remove redundant information, we conducted a correlation analysis on 19 bioclimatic variables. We excluded the bioclimatic variables that had a correlation coefficient greater than 0.8^{32,33}.

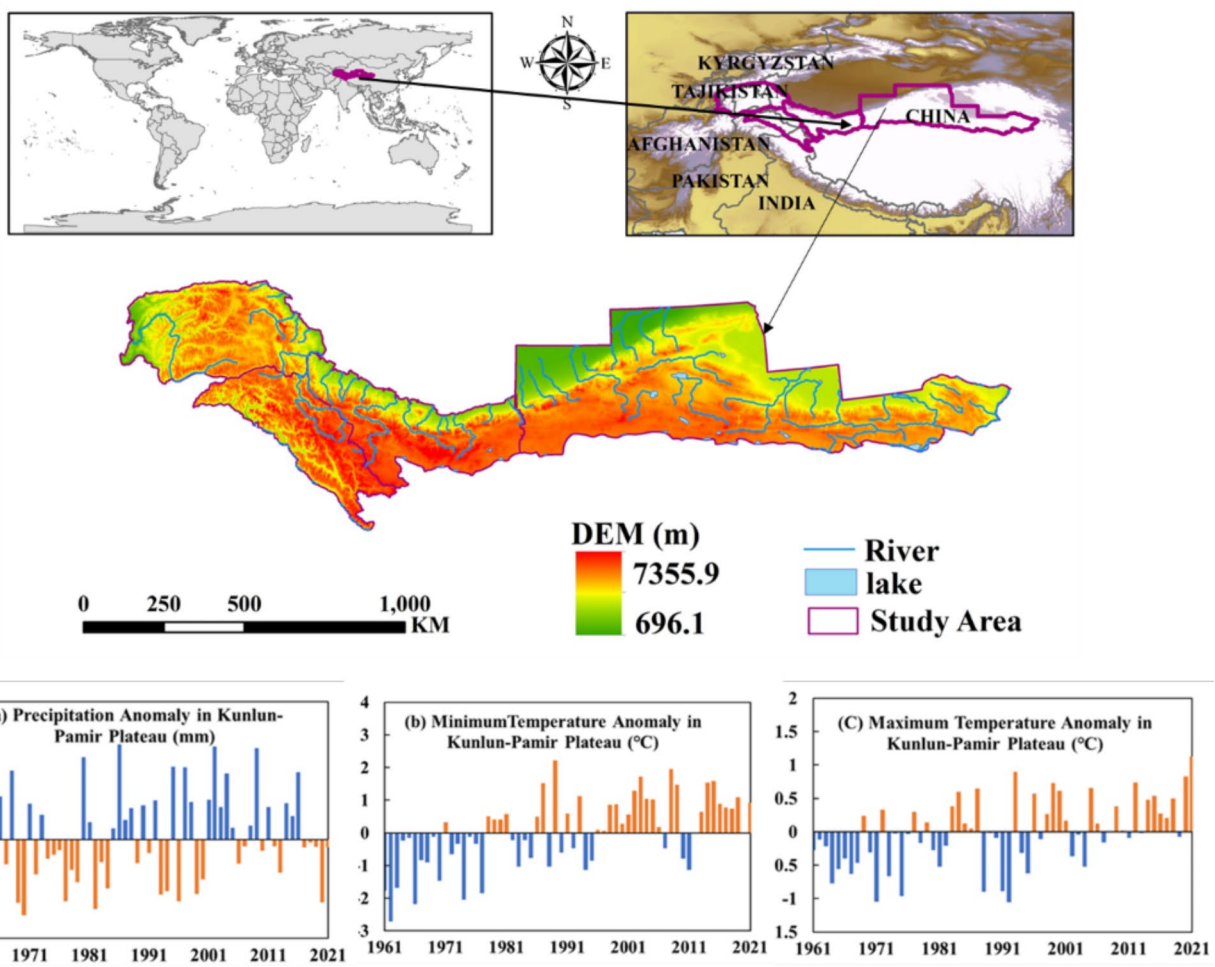


Fig. 1. Characteristics of the Kunlun-Pamir Plateau including (a) Precipitation anomaly, (b) Minimum Temperature anomaly and (c) Maximum Temperature anomaly from 1961 to 2022. PP, KK, WK and EK refer to Pamir Plateau, Karakoram, West KunLun, and East KunLun, respectively.

Theil-Sen median slope

The Theil-Sen median slope is a nonparametric method for detecting trends in time series data. This approach does not require the measurements to conform to a positively trending distribution, is robust against missing values and outliers, and is well-suited for conducting trend significance tests on long time series datasets^{33–35}. We utilized Theil-Sen median slope to assess the changing trends of the 19 bioclimatic variables.

$$T_{slope} = \text{median} \left(\frac{x_j - x_i}{j - i} \right), \forall i < j \quad (1)$$

T_{slope} indicates the slope of bioclimatic variables. x_i and x_j indicates the annual average of 19 bioclimatic variables separately for the i -th and j -th years. When $T_{slope} > 0$, it indicates an upward trend in bioclimatic variables during the study period, conversely, it indicates a decrease. The larger the absolute value, the greater the degree of bioclimatic variables change. When $T_{slope} = 0$, it signifies those bioclimatic variables remains essentially unchanged during the study period.

Empirical orthogonal function

Empirical Orthogonal Function (EOF) decomposition is a multivariate statistical analysis technique that identifies and extracts significant spatial-temporal modes from high-dimensional datasets. In climate science, EOF analysis reveals the intrinsic structure of climate variables by decomposing complex climate signals into a series of orthogonal modes, which are ordered by their variance contributions. Each mode is linked to a specific principal component time series, enabling researchers to quantify and interpret the dominant variability in climate data. EOF decomposition is not only instrumental in identifying the key drivers of the climate system, but it also plays a crucial role in predicting climate trends and assessing the impacts of climate change³⁶. Although the eigenvectors obtained from EOF decomposition do not indicate the magnitudes of bioclimatic variables, the use of the EOF decomposition method produces distinctive vectors that mirror the spatial distribution patterns

Types	Variables	description	Units
Energy factors	BIO1	Annual Mean Temperature	°C
	BIO2	Mean Diurnal Range	°C
	BIO3	Isothermality	–
	BIO4	Temperature Seasonality	–
	BIO5	Max Temperature of Warmest Month	°C
	BIO6	Min Temperature of Coldest Month	°C
	BIO7	Temperature Annual Range	°C
	BIO8	Mean Temperature of Wettest Quarter	°C
	BIO9	Mean Temperature of Driest Quarter	°C
	BIO10	Mean Temperature of Warmest Quarter	°C
Water factors	BIO11	Mean Temperature of Coldest Quarter	°C
	BIO12	Annual Precipitation	mm
	BIO13	Precipitation of Wettest Month	mm
	BIO14	Precipitation of Driest Month	mm
	BIO15	Precipitation Seasonality	–
	BIO16	Precipitation of Wettest Quarter	mm
	BIO17	Precipitation of Driest Quarter	mm
	BIO18	Precipitation of Warmest Quarter	mm
	BIO19	Precipitation of Coldest Quarter	mm

Table 1. Definitions of 19 bioclimatic variables used in this study.

of changes in such variables. There is no absolute meaning to the positive or negative values of the eigenvectors, but they are relative to the phase of the eigenvectors. Time coefficients are used as weights for spatial patterns. A higher absolute value of the time coefficient indicates the more typical distribution for that year^{36–38}. In the Kunlun–Pamir Plateau, a region characterized by complex topography and variable climate, EOF analysis serves as an effective tool for extracting the primary spatial distribution characteristics and temporal variation patterns of climate variables. This analysis can enhance our understanding of the climate patterns and their changes within the region.

$$C_{m \times m} = \frac{1}{n} (X_{m \times n} \times X_{m \times n}^T) \quad (2)$$

The eigenvalues ($\lambda_1, \lambda_2, \dots, \lambda_m$) of the matrix $C_{m \times m}$ and the eigenvectors $V_{m \times m}$ satisfy:

$$C_{m \times m} \times V_{m \times m} = V_{m \times m} \times E_{m \times m} \quad (3)$$

$$E_{m \times m} = \begin{pmatrix} \lambda_1 & & 0 \\ & \ddots & \\ 0 & & \lambda_m \end{pmatrix} \quad (4)$$

Obtain the time coefficient matrix $T_{m \times m}$:

$$T_{m \times n} = V_{m \times m}^n \times X_{m \times n} \quad (5)$$

The variance contribution rate of the k -th mode is:

$$\text{variance contribution} = \frac{\lambda_k}{\sum_{i=1}^m \lambda_i} \times 100\% \quad (6)$$

In this paper, the North method is employed to conduct a significance test on the error range of eigenvalues. The error of eigenvalues at a 95% confidence level is:

$$\Delta \lambda = \lambda \sqrt{\frac{2}{N}} \quad (7)$$

In the equation: λ represents eigenvalues, and N is the total sample size. λ is examined sequentially, and error ranges are assigned. If there is no overlap in the error range between two adjacent eigenvalues, i.e., the upper limit of the error for λ_{i+1} is smaller than the lower limit of the error for λ_p , it indicates a test pass.

Wavelet analysis

Wavelet analysis offers advantages over multiscale analysis, capturing local features and frequency changes in time series data^{39,40}. The Morlet-based continuous wavelet analysis method was employed to uncover the periodic traits of the 19 bioclimatic variables at various temporal intervals. The following equation defines the Continues Wavelet Transform (CWT):

$$W_n^x s = \sum_{n=0}^{N-1} x_n \Psi^* \frac{n' - ndx}{s} \quad (8)$$

where x_n denotes a discrete sequence of observations, with n as the localized time index. N represents the signal's length, while S signifies the wavelet scale and dx stands for the sampling interval. Ψ denotes the wavelet function, which has been scaled and translated, and the $*$ symbolizes the complex conjugate.

To address uncertainty propagation, we first normalize and detrend the data to minimize the influence of noise and trends on the analytical results. Next, we tackle boundary effects by introducing a cone of influence (COI), ensuring that only regions unaffected by these effects are analyzed^{40,41}. We further employ significance tests to identify statistically significant regions, enabling us to differentiate between genuine periodic signals and noise. Finally, we incorporate global wavelet spectral analyses to quantify the major periodic features within the time series. Through these methodologies, we effectively manage the uncertainty propagation issue and enhance the robustness of our analytical results.

Results

Correlation of bioclimatic variables

The correlation coefficient between Annual Mean Temperature and Mean Temperature of Warmest Quarter was 0.84, between Annual Precipitation and Precipitation of Wettest Month was 0.81, between Annual Precipitation and Precipitation of Wettest Quarter was 0.87, and between Precipitation of Wettest Month and Precipitation of Wettest Quarter was 0.91. Therefore, the retained variables were BIO1–9, Annual Precipitation, BIO14–15, and BIO17–19, totalling 15 bioclimatic variables (Fig. 2).

Inter-annual variation of bioclimatic variables

From 1961 to 2022, the trends of bioclimatic variables related to energy factors (BIO1–9) were significant ($P < 0.05$). Among them, Annual Mean Temperature, Max Temperature of Warmest Month, Min Temperature of Coldest Month, Mean Temperature of Wettest Quarter, and Mean Temperature of Driest Quarter showed significant increasing trends (Fig. 3). Mean Diurnal Range $^{-4}$ and Temperature Annual Range exhibited significant decreasing trends. Among them, Min Temperature of Coldest Month had the fastest increasing rate at $0.037\text{ }^{\circ}\text{C/a}$, followed by Mean Temperature of Driest Quarter with an increasing rate of $0.032\text{ }^{\circ}\text{C/a}$. The fastest decreasing rate for Temperature Seasonality was $0.49\text{ }^{\circ}\text{C/a}$. This indicated that the overall temperature in the Kunlun–Pamir Plateau was gradually increasing, with an increase in minimum temperatures during winter, and a reduction in temperature differences between different seasons. It can be inferred that the decrease in the slope of Isothermality is due to the slope of Temperature Annual Range ($-0.026\text{ }^{\circ}\text{C/a}$) being smaller than the slope of Mean Diurnal Range ($-0.016\text{ }^{\circ}\text{C/a}$) (Fig. 3). The reason for the decrease in the slope of Temperature Annual Range was that the rate of increase in Max Temperature of Warmest Month ($0.011\text{ }^{\circ}\text{C/a}$) was higher than the rate of increase in Min Temperature of Coldest Month ($0.037\text{ }^{\circ}\text{C/a}$).

In terms of water factors, except for Precipitation Seasonality, which showed a significant decreasing trend ($P < 0.05$), other bioclimatic variables exhibited significant increasing trend except Precipitation of Coldest Quarter which showed non-significant increasing (Fig. 3). Among them, Annual Precipitation had the fastest increasing rate of 0.33 mm/a , followed by Precipitation of Driest Quarter with a rate of 0.04 mm/a . This indicated that the differences in precipitation between different seasons in the Kunlun–Pamir Plateau had not significantly decreased. The region showed an increasing trend in annual precipitation, with an increase in rainfall during the driest quarter. Overall, the indicators directly reflecting climate fluctuations, such as Mean Diurnal Range, Isothermality, Temperature Seasonality, Temperature Annual Range and Precipitation Seasonality, all exhibited a decreasing trend in the time series. This suggested that the climate fluctuations in the study region have been decreasing.

Spatial variation of bioclimatic variables

Bioclimatic variables exhibited spatial heterogeneity in the Kunlun–Pamir Plateau (Fig. 4). In terms of energy factors, both Annual Mean Temperature and Min Temperature of Coldest Month showed an increasing trend in spatial distribution, with higher values mainly concentrated in the northwest part of the eastern Kunlun–Pamir Plateau. Lower values were observed in the east KunLun, Karakoram, and the northwest part of Pamir. Mean Diurnal Range, Temperature Seasonality, and Temperature Annual Range all exhibited a decreasing trend. The regions with the fastest decreasing trends were the West KunLun and the Karakoram. Temperature Seasonality also showed a fast-decreasing trend in the western part of the East KunLun. This indicates that interannual and seasonal variability in the Kunlun–Pamir Plateau has decreased overall, but regional changes exhibit spatial heterogeneity. For Isothermality, Max Temperature of Warmest Month, Mean Temperature of Wettest Quarter, and Mean Temperature of Driest Quarter, there were both increasing and decreasing trends. The areas with high values of increasing trends were mainly concentrated in the western and central parts of the East KunLun. The areas with high values of decreasing trends for Isothermality and Max Temperature of Warmest Month were mainly distributed in the Karakoram and the West KunLun. Most of the areas with a decreasing trend for Mean Temperature of Wettest Quarter were mainly distributed in the central and western parts of the Pamir Plateau,

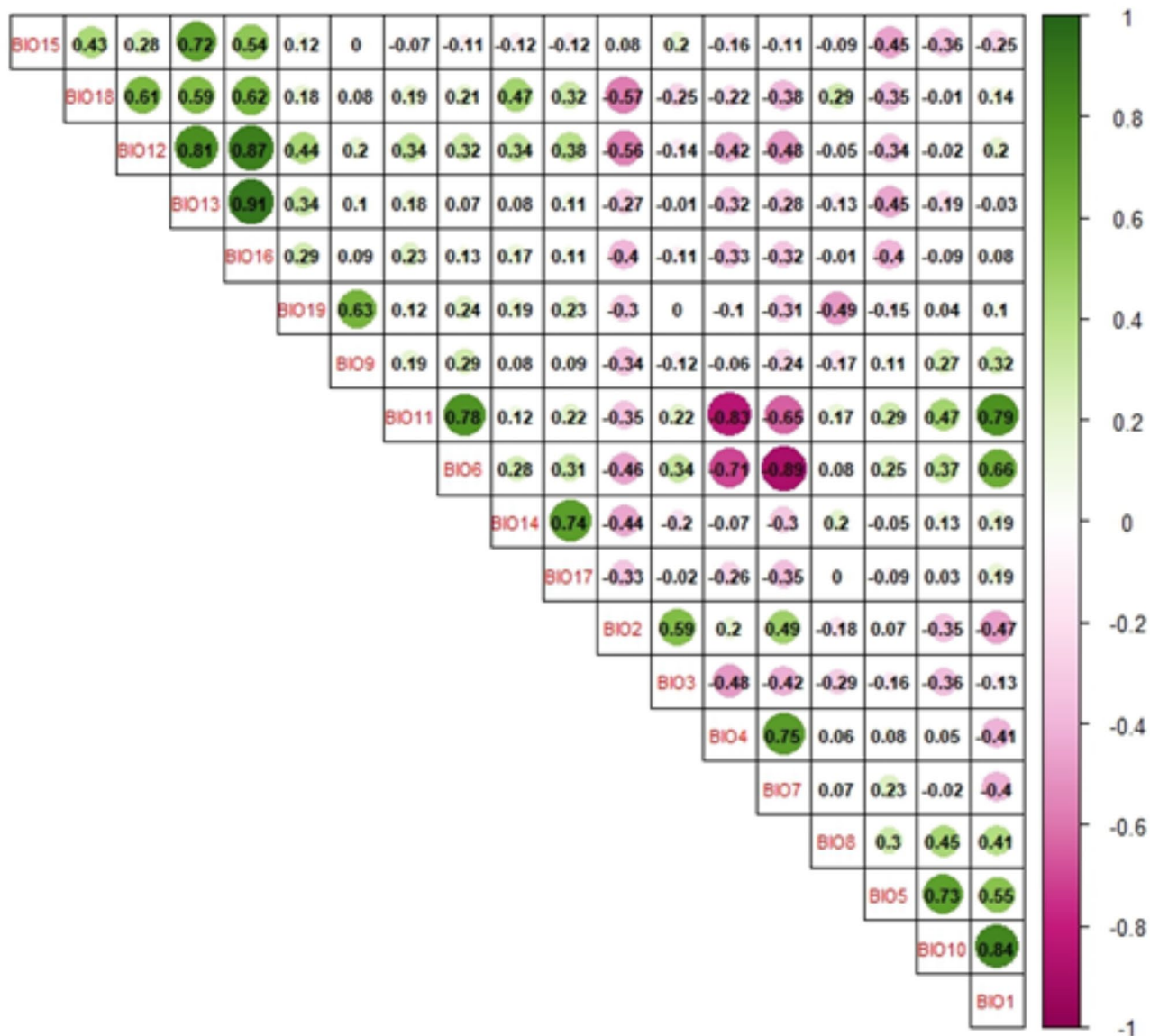


Fig. 2. Correlation of bioclimatic variables from 1961 to 2022.

while only a few areas showed a decreasing trend for Mean Temperature of Driest Quarter. Overall, the areas with increased trends of bioclimatic variables related to energy factors were mainly concentrated in the western part of the East KunLun. On the other hand, the West KunLun was the focal area for the decreasing trends of bioclimatic variables.

In terms of water factors, Annual Precipitation, Precipitation of Driest Month, Precipitation Seasonality, Precipitation of Driest Quarter, Precipitation of Warmest Quarter, and Precipitation of Coldest Quarter also exhibited spatial heterogeneity (Fig. 4). Except for Precipitation Seasonality, the areas with high values of increasing trend for the other bioclimatic variables were mainly concentrated in the Pamir and the Karakoram. The high values of increasing slopes for Precipitation Seasonality were mainly concentrated in the central parts of the West KunLun and the East KunLun, indicating that these two areas might be prone to extreme climate events. The areas with high decreased trend were mainly distributed in the western part of the East KunLun.

Dominant pattern of bioclimatic variables

The variance contribution rates corresponding to the first two eigenvectors of the 19 bioclimatic variables were shown in Table 2. For the first two EOFs of the 15 bioclimatic variables except for Mean Temperature of Wettest Quarter, Mean Temperature of Driest Quarter, Precipitation Seasonality, explained over 50% of the total variance, the variance contribution rates of the first two modes of Mean Temperature of Wettest Quarter, Mean Temperature of Driest Quarter, Precipitation Seasonality are 46%, 37%, and 46% respectively. The error ranges of the first two characteristic roots did not overlap and passed the North significance test⁴². They were therefore identified for subsequent discussion and analysis.

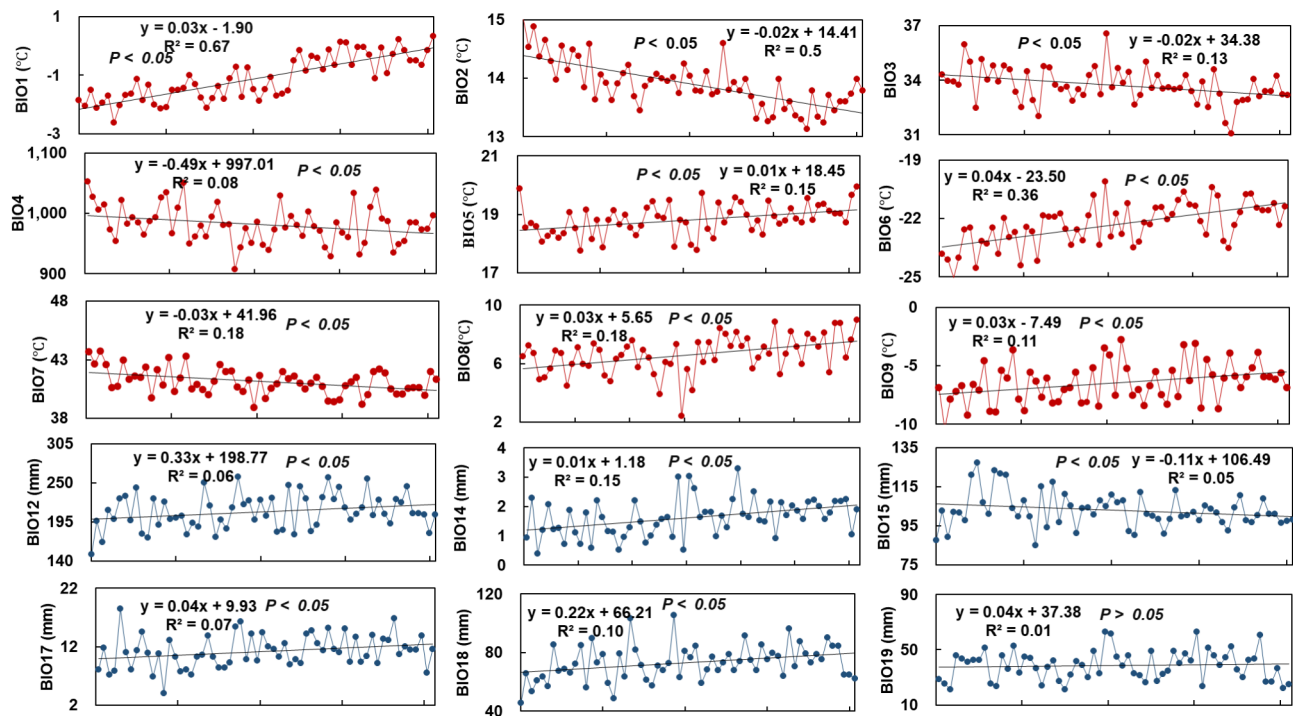


Fig. 3. Interannual variations in bioclimatic variables from 1961 to 2022.

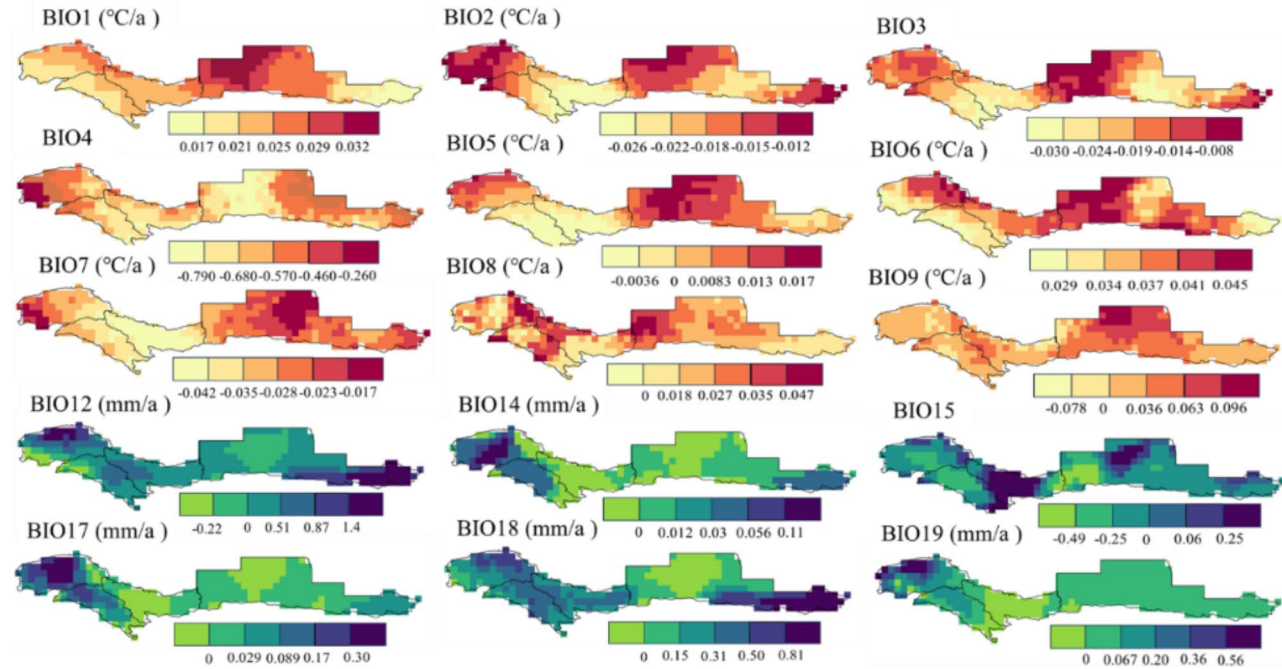


Fig. 4. Spatial patterns of trends in bioclimatic variables.

The spatial pattern of EOF1 for bioclimatic variables is shown in (Fig. 5) and the time coefficients of EOF1 are shown in (Fig. 6). In terms of energy factors, Annual Mean Temperature, Isothermality, and Min Temperature of Coldest Month all exhibited positive values, indicating a consistent trend in the region. Moreover, the high values of EOF1 were in the Pamir Plateau and the West KunLun, indicating that these three bioclimatic variables have the highest variability in these regions. Furthermore, Annual Mean Temperature and Min Temperature of Coldest Month exhibited high values in the western part of the East KunLun. Isothermality showed significant intensity variation in the central Kunlun Mountains. The first principal component (PC1) of Annual Mean

Bioclimatic variables	The first mode (EOF1) variance contribution rate/%	The second mode (EOF2) variance contribution rate/%	Cumulative variance contribution rate/%
BIO1	83	10	93
BIO2	68	11	79
BIO3	54	26	80
BIO4	64	26	90
BIO5	49	33	82
BIO6	66	21	87
BIO7	55	26	81
BIO8	34	12	46
BIO9	25	12	37
BIO12	56	12	68
BIO14	56	10	66
BIO15	31	15	46
BIO17	59	15	74
BIO18	31	23	54
BIO19	76	10	86

Table 2. Percentage of variance explained by the first two varimax loadings (EOFs) of bioclimatic variables from 1961 to 2022.

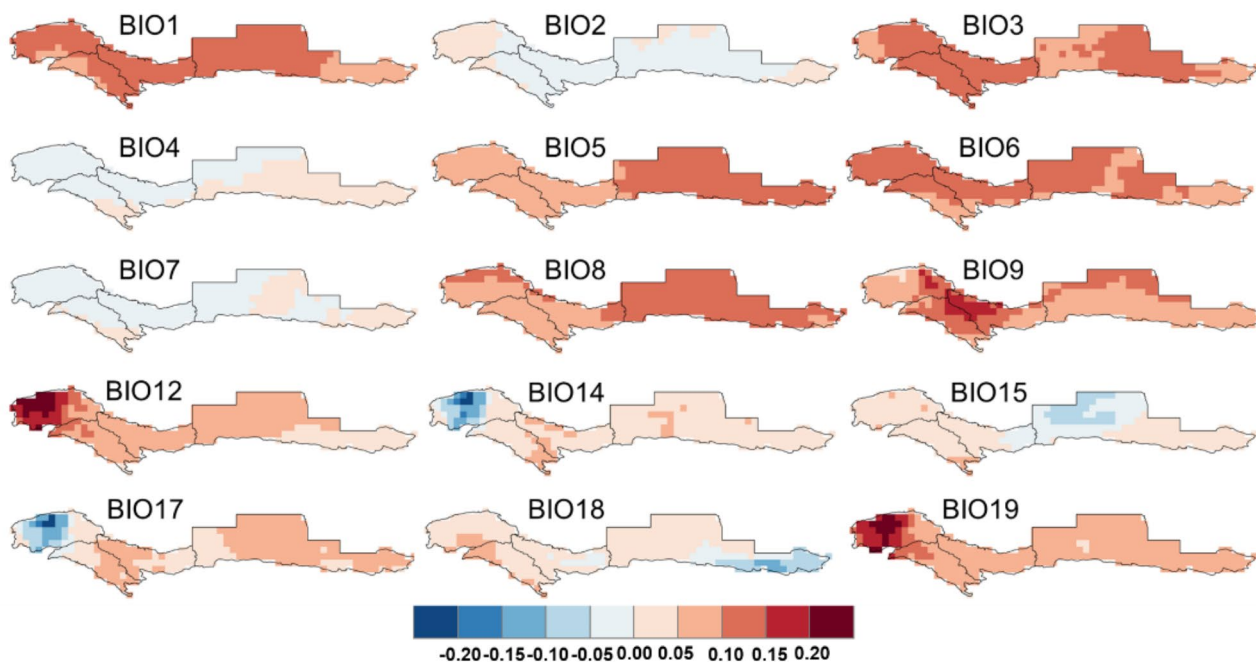


Fig. 5. Spatial patterns of EOF1 over the Kunlun–Pamir Plateau region during 1961–2022.

Temperature underwent an abrupt shift in 1997, with negative phase dominating before and positive phase prevailing thereafter. The time coefficient of Isothermality was mainly positive and gradually transitioned to predominantly negative values contrary to Min Temperature of Coldest Month, indicating that the temperature fluctuations have increased in the Kunlun–Pamir Plateau, and that the lowest temperatures in the coldest months have been rising. Max Temperature of Warmest Month and Mean Temperature of Driest Quarter had very few negative values, but the majority of regions showed consistent changes. From the time coefficients, it can be observed that for Max Temperature of Warmest Month and Mean Temperature of Driest Quarter, the predominant negative values gradually transitioned to predominantly positive values. This indicated that in the Kunlun–Pamir Plateau, the highest temperatures during the warmest months were increasing, and the average temperatures during the driest season were also rising. The presence of both positive and negative values in the EOF1 of Mean Diurnal Range, Temperature Seasonality, Temperature Annual Range, and Mean Temperature of Wettest Quarter indicated that these four bioclimatic variables exhibited spatial heterogeneity. However, its values were relatively small, indicating that these four bioclimatic variables had relatively small fluctuations across the

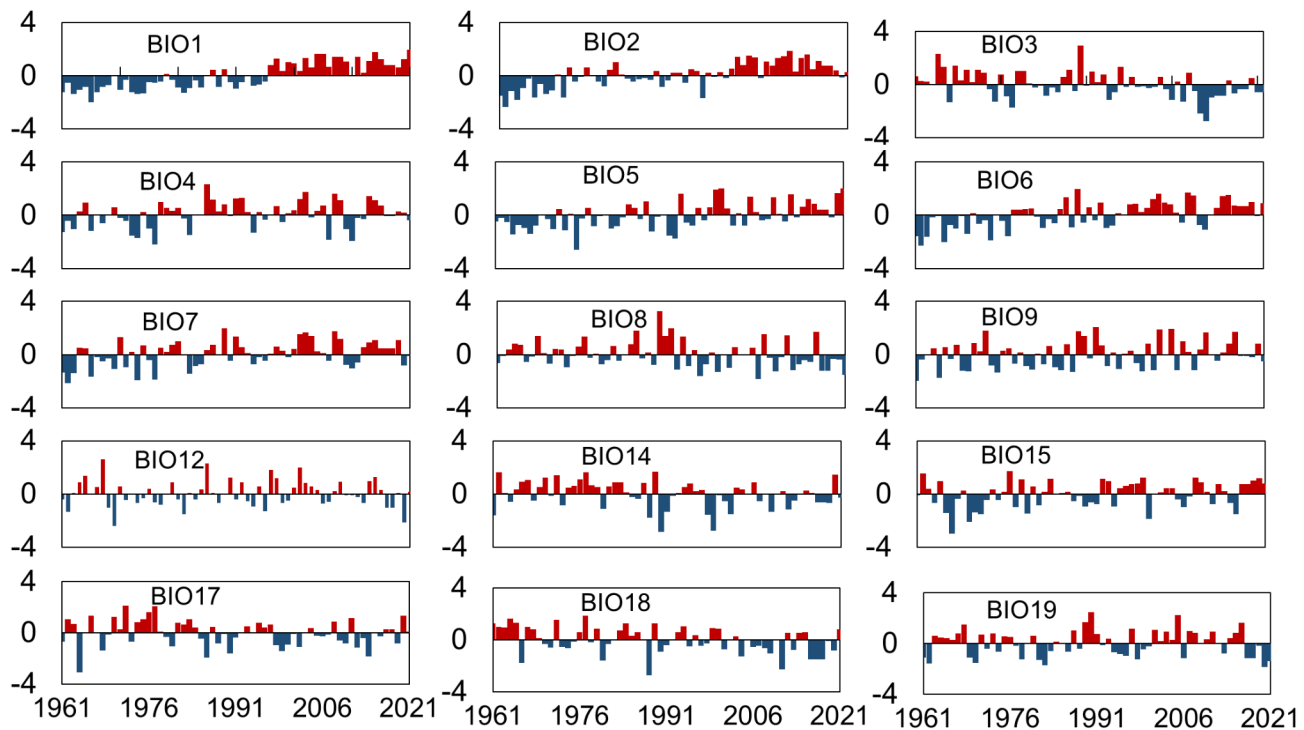


Fig. 6. Time coefficients of EOF1 over the Kunlun–Pamir Plateau region during 1961–2022.

region. The time coefficients of Mean Diurnal Range, Temperature Seasonality, and Temperature Annual Range were initially dominated by negative values and gradually shifted towards positive values. This indicated that the corresponding EOF1 represented an increasing number of years with a positive spatial pattern. The time coefficients of BIO8 showed an increasing trend of negative values, indicating that over the years, there was an increasing occurrence of the negative spatial pattern represented by the current EOF1 of Mean Temperature of Wettest Quarter. In the water factors, all six BIO variables (Annual Precipitation, Precipitation of Driest Month, Precipitation Seasonality Precipitation of Driest Quarter, Precipitation of Warmest Quarter, Precipitation of Coldest Quarter) in EOF1 exhibited both positive and negative values, indicating the non-uniform changes of the biological climatic variables in the Kunlun–Pamir Plateau. However, for Annual Precipitation and Precipitation of Coldest Quarter, there were only a few regions with negative values, and these were almost invisible in the figure. Moreover, the high-value centers of Precipitation of Driest Month and Precipitation of Wettest Quarter were mainly distributed in the western part of the Kunlun–Pamir Plateau, while the low-value centers of Precipitation of Driest Month and Precipitation of Wettest Quarter were in the western part of the Pamir. The low-value center of Precipitation Seasonality is situated in the western part of the East KunLun, and the low-value center of Precipitation of Warmest Quarter was in the eastern part of the East KunLun. The occurrence of high-value and low-value centers in these regions indicated that the corresponding variables exhibited significant fluctuations in these areas. From the time series perspective, the distribution patterns of Annual Precipitation and Precipitation of Coldest Quarter showed no significant changes. The increasing number of negative values in Precipitation of Driest Month, Precipitation of Driest Quarter, and Precipitation of Warmest Quarter, along with the larger absolute values of their time series, indicated a mitigated decreasing trend in precipitation during the driest month, the driest quarter, and the coldest season in the eastern part of the Pamir Plateau. This suggested that the moisture in the region may be increasing. Bioclimatic variables EOF2 (Figs. 7 and 8) showed predominantly positive values in most regions of the Kunlun–Pamir Plateau indicating the consistency of variations in biological climate variables in this region. In summary, the above analyses suggested that the first two EOFs can represent the dominant patterns of bioclimatic variables in the Kunlun–Pamir Plateau.

Cyclical characteristics of bioclimatic variables

Figure 9 and Table 3 depict the temporal variations of a range of bioclimatic variables, examined within a 95% confidence interval. The Mean Diurnal Range exhibited a cycle ranging from 1 to 3 years, specifically during 1968–1975. Isothermality revealed distinct period scales of 1–5 years and 8–13 years, corresponding to the intervals of 1962–1980 and 1970–2013, respectively. This indicates Isothermality's temporal variability, marked by alternating shifts between shorter and longer periods. Temperature Seasonality displayed a broader period scale of 2–16 years, spanning from 1972 to 2015. Precipitation Seasonality was characterized by a longer period scale of 3–6 years, noted from 1968 to 1975.

In general, almost all bioclimatic variables, with the exception of BIO1, demonstrated periods of 1–4 years, though the specific years of occurrence varied. Variables such as Isothermality, Min Temperature of Coldest Month, Temperature Annual Range, Mean Temperature of Wettest Quarter, and Mean Temperature of Driest

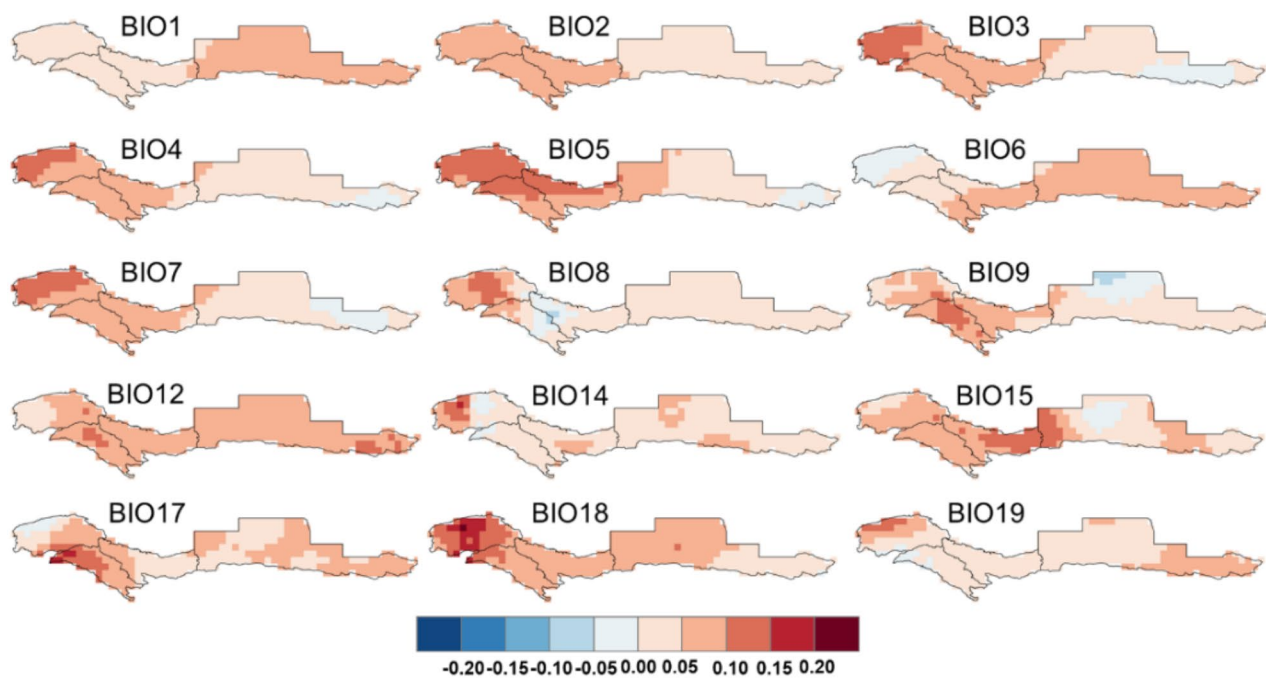


Fig. 7. Spatial patterns of EOF2 over the Kunlun–Pamir Plateau region during 1961–2022.

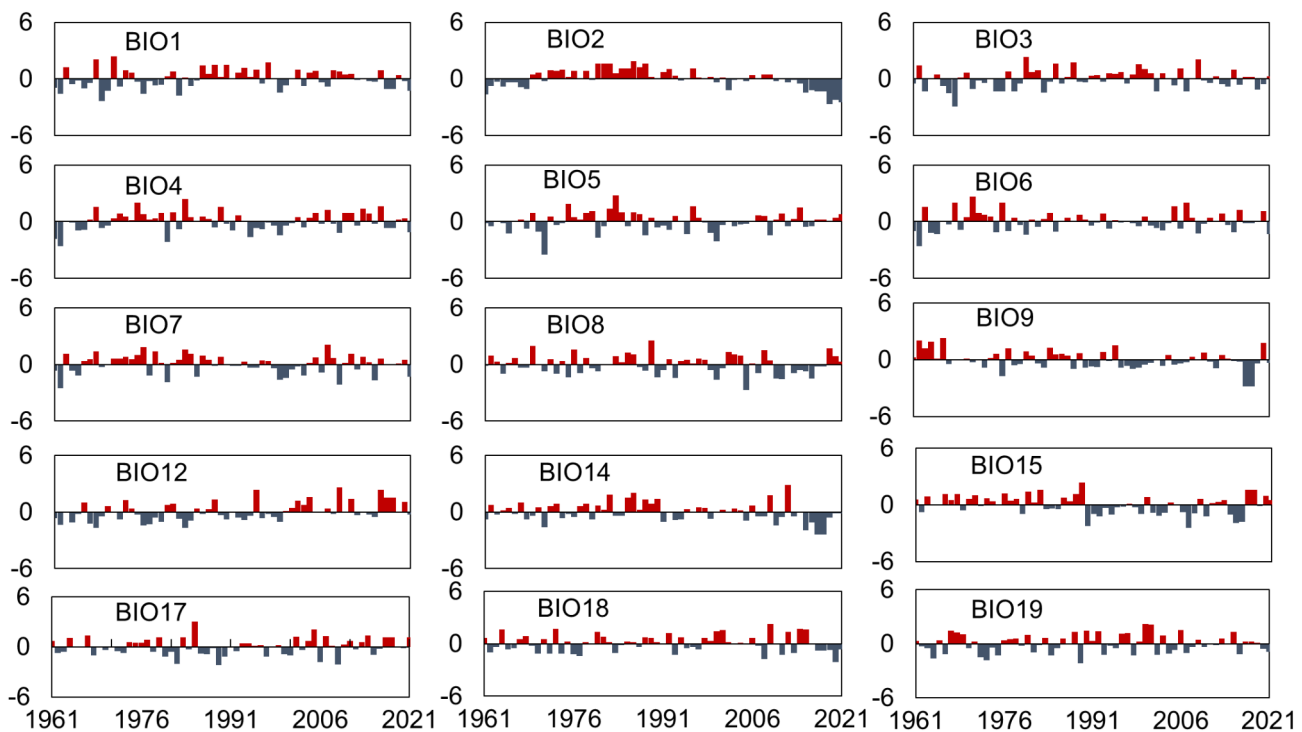


Fig. 8. Time coefficients of EOF2 over the Kunlun–Pamir Plateau region during 1961–2022.

Quarter showed a pattern of fluctuating periods, transitioning from short to long cycles and then reverting to shorter cycles. This pattern suggests a dynamic process of transition in bioclimatic variables, moving from rapid to slower variations.

Notably, several variables including Annual Mean Temperature, Mean Diurnal Range, Max Temperature of Warmest Month, Precipitation of Driest Month, Precipitation Seasonality, Precipitation of Driest Quarter,

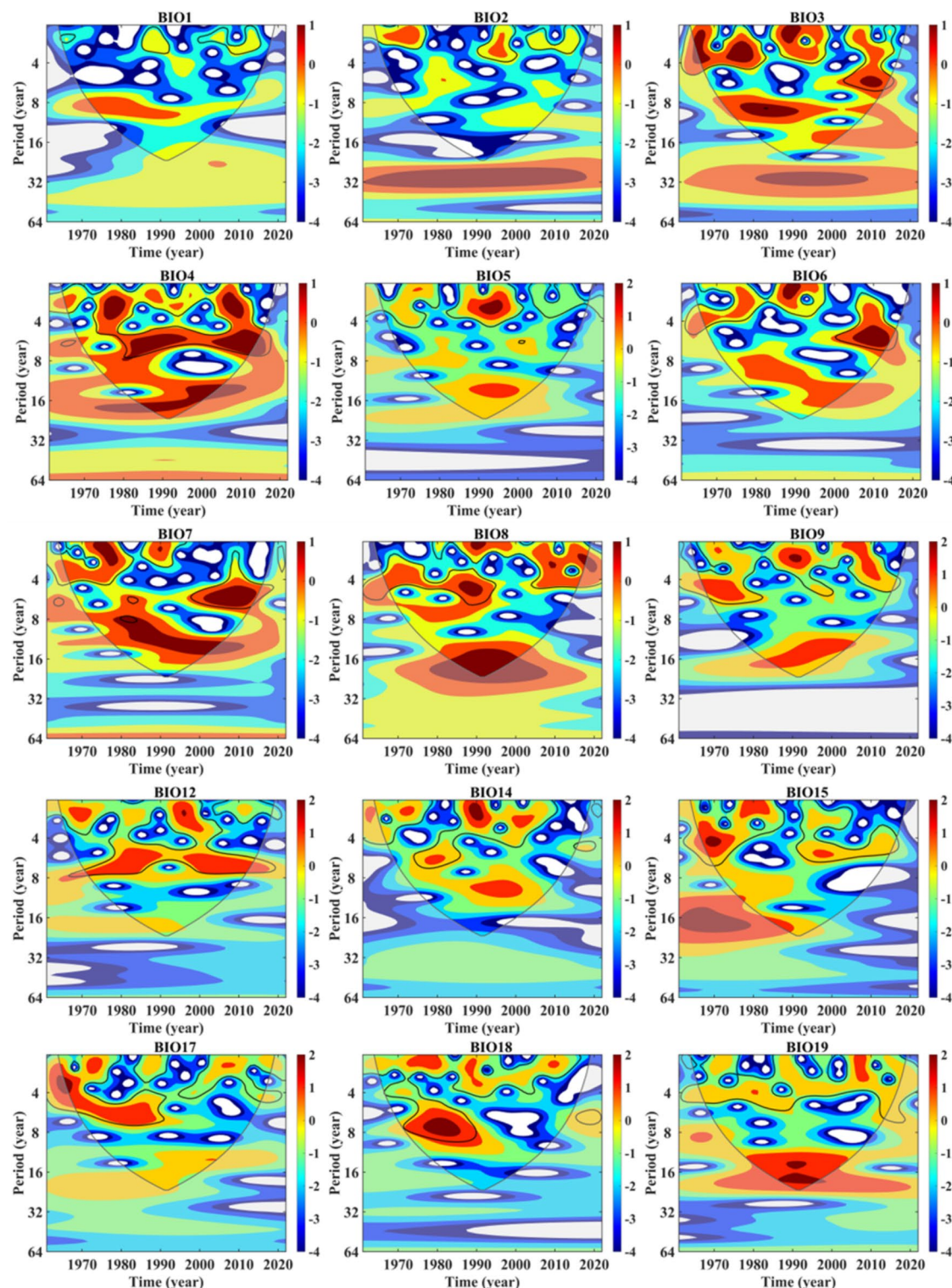


Fig. 9. Continuous Wavelet Power Spectrum of bioclimatic variables in the Kunlun–Pamir Plateau from 1961 to 2022 (the black line was the critical line of the COI, which indicated the region where the edge effect of continuous wavelet transformed data had a greater impact).

Bioclimatic variables	Period scale (years)	Corresponding year
BIO1	8–12	1968–1998
BIO2	1–3	1968–1975
BIO3	1–5	1962–1980
	8–13	1970–2013
BIO4	2–16	1972–2015
BIO5	2–5	1985–2000
BIO6	1–5	1967–1978
	3–8	1977–2015
	8–16	2000–2018
BIO7	1–5	1964–1980
	3–8	1995–2015
	5–16	1970–2005
BIO8	3–8	1961–1992
	16–20	2005–2022 (1980–2005)
BIO9	4–5	1968–1978
	12–18	1985–2008
	1–5	2007–2012
BIO12	1–2	1968–1971
	5–9	1963–1990
	1–4	1998–2018
BIO14	1–4	1988–1994
BIO15	3–6	1968–1975
BIO17	2–7	1962–1988
BIO18	5–9	1970–1990
BIO19	14–20	1978–2015

Table 3. Period Scale of 19 bioclimatic variables.

Precipitation of Warmest Quarter, and Precipitation of Coldest Quarter did not exhibit significant periodic trends in the last 2 decades.

Discussion

Changes in climate fluctuations in the Kunlun–Pamir plateau

Our research shows that climate variability in the region has steadily decreased from 1961 to 2022 (Figs. 3 and 4). These findings align with previous research and emphasize the susceptibility of mountainous areas to climate change and regional climate fluctuations⁴³. Our research revealed that the decrease in energy-related factors, Mean Diurnal Range, Isothermality, Temperature Seasonality, and Temperature Annual Range, can be attributed to the higher rate of increase in the lowest temperature of the coldest month (Min Temperature of Coldest Month) compared to the highest temperature of the hottest month (Max Temperature of Warmest Month) (Figs. 3 and 4). The negative slope of Isothermality indicates a gradual decrease in the temperature difference between day and night. Similarly, the negative slope of Temperature Seasonality suggests that seasonal temperature variations are becoming less extreme, with diminishing differences between temperatures across various seasons. In relation to Temperature Annual Range, which represents the difference between the average temperatures of the hottest and coldest months of the year, a negative slope indicates a reduction in this range. This implies that the gap between the highest and lowest temperatures throughout the year is narrowing, reflecting a less extreme climate. Furthermore, the negative slope of Precipitation Seasonality signifies that the variation in precipitation across different seasons is becoming less pronounced. In other words, the difference between the wettest and driest periods of the year is decreasing, leading to a more even distribution of rainfall throughout the year. This trend suggests a movement towards a more consistent or balanced precipitation pattern across the seasons. This discovery is consistent with a previous study⁴⁴. Despite a decrease in climate variability, the rise in the highest temperature of the hottest month (Max Temperature of Warmest Month) and the increase in the lowest temperature of the coldest month (Min Temperature of Coldest Month) on the Kunlun–Pamir Plateau (Figs. 1 and 4) have led to a reduction in snow cover area and a decrease in the fraction of snowfall. As a result, this has impacted changes in water resources in the region⁴⁵. Furthermore, the increase in temperature coupled with elevated precipitation has led to an advancement in the phenology of vegetation in this region⁴⁶. However, it's important to note that the temperature rise has also intensified glacier melting, consequently raising the risk of glacial lake outburst floods in the study region⁴⁶.

Comparative analysis with the Tibetan Plateau Plateau

The Kunlun–Pamir Plateau and the Tibetan Plateau are not clearly delineated in the current study. In this research, the Kunlun–Pamir Plateau is considered the northern and northwestern extension of the Tibetan

Plateau, highlighting their close geological, geographical, and climatic relationships. The Kunlun Mountains, which serve as the northern boundary of the Tibetan Plateau, along with the Pamir Plateau, create a natural barrier to the northwestern part of the Tibetan Plateau. Collectively, this series of plateaus has significantly influenced the climatic patterns of the Asian continent, with extensive implications for the region's hydrology and ecosystems. Previous studies have demonstrated that the Tibetan Plateau is experiencing a significant warming and humidifying trend⁴⁷, aligns with the findings from our research conducted in the Kunlun–Pamir Plateau. Both the Annual Mean Temperature and Annual Precipitation have shown an increasing trend (Fig. 3). The plateau warms more during the night than during the day, resulting in a decrease in the daily temperature difference⁴⁸, which is also consistent with our research (Fig. 3). However, due to the influence of topography and other factors, the climate change in the Kunlun–Pamir region and the Tibetan Plateau showed spatial heterogeneity^{49,50}. Besides, Li et.al (2023) proved climate cyclicity in Southeast Tibet shows a clearer and more consistent pattern of long cycles, reflecting the relative stability and regularity of the climate system in the region⁵¹. In contrast, climate change on the Kunlun–Pamir Plateau shows more complex short-cycle fluctuations and a shift from rapid to slow changes. This may be related to the different geographical locations, topographic features and climatic backgrounds of the two areas.

The Kunlun–Pamir Plateau, shaped by rugged terrain and westerly winds, experiences a more arid climate⁵², while the Tibetan Plateau, influenced by the Indian monsoon, receives higher precipitation⁵³. Their elevation differences further impact atmospheric circulation, with the Tibetan Plateau intensifying monsoonal activity^{53,54} and the Kunlun–Pamir Plateau exhibiting unique glacial and hydrological dynamics^{55,56}.

Understanding these differences is important for the prediction of regional climate change and the development of response measures. Furthermore, there is a notable lack of comprehensive studies analyzing the Tibetan Plateau through the lens of bioclimatic variables. Such analyses could be conducted in future research to enhance the ecological protection of the Tibetan Plateau.

Ecological consequences of climate fluctuations in the Kunlun–Pamir Plateau

This study investigates the spatial heterogeneity of the Kunlun–Pamir Plateau by analyzing climatic fluctuations from 1961 to 2022 using 19 bioclimatic variables. Our results indicate a decline in Mean Diurnal Range, Isothermality, Temperature Seasonality, and Temperature Annual Range suggesting a weakening of climatic fluctuations in this plateau. Conversely, in the western part of the Kunlun Mountains, we observed an increasing trend in mean annual temperature and precipitation seasonality, indicating enhanced localized climate fluctuations in that region (Figs. 3 and 4). Climate change significantly influences species distribution in mountainous regions⁵⁷. On the Kunlun–Pamir Plateau, species richness exhibits a strong correlation with climatic factors⁵⁸, underscoring the necessity of understanding climate variability's impacts on the region's ecosystems. Previous studies have demonstrated mammal distribution changes are indeed caused by temperature^{59–61}. For instance, Li et al. (2019) found that the probability of Marco Polo sheep distribution significantly increased as the range of seasonal temperature variation diminished⁶¹. This finding aligns with the observed decreasing trends in temperature seasonality and annual temperature range in our study, suggesting that reduced climatic fluctuations may create a more stable habitat for these species.

Moreover, it has been reported that species richness is increasing in the Kunlun–Pamir Plateau^{62,63}, potentially due to changes in climatic conditions. Empirical orthogonal function (EOF) analyses reveal the complexity of this variability (Figs. 5 and 6), with EOF2 for isotherms, temperature seasonality, annual temperature variability range, and precipitation seasonality predominantly exhibiting positive values (Figs. 7 and 8). This suggests that the variability is heterogeneous across the plateau, providing suitable habitats for various species and thereby explaining the rise in species diversity in the region⁶⁴. Furthermore, despite an overall decrease in climatic fluctuations, the seasonal increase in Annual Mean Temperature and precipitation in localized areas of the western Kunlun Mountains may have contributed to changes in the local distribution of species, further enriching the area's biodiversity^{65,66}.

The study reveals that the Kunlun–Pamir Plateau is experiencing complex climatic shifts, with bioclimatic variables showing 1- to 4-year cycles and a notable transition in Isothermality and temperature annual range from short to long cycles (Fig. 9 and Table 3), indicating a shift from rapid to slower climate variations. These changes further suggest more stable but gradually altering environmental conditions, which could impact species distribution and biodiversity⁶⁵. Specifically, reduced temperature seasonality appears to support a more predictable habitat for species like the Marco Polo sheep, while localized increases in temperature and precipitation seasonality in the western Kunlun Mountains may lead to microhabitat differentiation, further enriching the region's biodiversity⁵⁹. These findings emphasize the need for ongoing climate monitoring to understand and predict the ecological consequences of these changes in mountainous regions. Given the decrease in climatic variability, conservation efforts should focus on habitat protection, ecological connectivity, adaptive management, and species translocation to enhance ecosystem resilience. Species habitat models should incorporate long-term climate trends, optimize migration corridors, and remain dynamic to support biodiversity planning.

Limitations and outlook

This study has limitations because the bioclimatic variables were derived from precipitation, minimum temperature, and maximum temperature, possibly lacking a sufficient mechanistic interpretation for ecological research⁶⁷. Further research is needed to examine the factors that contribute to changes in bioclimatic variables across different regions, such as atmospheric circulation, climate system variations, and regional environmental characteristics. This will enhance understanding of the mechanisms driving these changes. Temperature and precipitation in mountainous areas frequently exhibit a correlation with altitude. Further research can provide a more detailed characterization of these patterns by focusing on the variation in altitude. The wavelet analysis

was conducted throughout the entire Kunlun–Pamir Plateau. Nevertheless, due to topography and geographical location, climate variability exhibited spatial heterogeneity across the Kunlun–Pamir Plateau.

Conclusion

This study analyzed climate variability in the Kunlun–Pamir Plateau from 1961 to 2022 using 19 bioclimatic variables, showing spatial heterogeneity. Energy factors like Mean Diurnal Range, Isothermality, Temperature Seasonality, and Temperature Annual Range indicated a decreasing trend in climate fluctuations across the plateau. Conversely, Annual Mean Temperature and Precipitation Seasonality increased in the western Kunlun Mountains, suggesting heightened climate fluctuations.

The trends of these bioclimatic variables were significant ($p < 0.05$), except for Precipitation of Wettest Month, all reflecting a general decrease in climate fluctuations. EOF analysis revealed that the first two EOFs of 15 bioclimatic variables explained over 50% of the total variance, showing significant variations and spatial heterogeneity. The EOF2 of Isothermality, Temperature Seasonality, Temperature Annual Range, and Precipitation Seasonality showed mostly positive values across the plateau, indicating non-uniform changes.

No significant periodicity was observed in these bioclimatic variables. Most had 1–4 year periods, but with different years of occurrence. Isothermality and Temperature Annual Range exhibited shifting patterns, transitioning from short to long cycles, indicating a shift from rapid to slower climate variations in the Kunlun–Pamir Plateau.

Data availability

The datasets generated during and/or analysed during the current study are available from the corresponding author upon reasonable request.

Received: 19 February 2024; Accepted: 7 April 2025

Published online: 17 April 2025

References

1. Beniston, M. Climatic change in mountain regions: A review of possible impacts. *Clim. Change* **59**(1), 5–31 (2003).
2. Palomo, I. Climate change impacts on ecosystem services in high mountain areas: A literature review. *Mt. Res. Dev.* **37**(2), 179–187 (2017).
3. Bede-Fazekas, Á. & Somodi, I. The way bioclimatic variables are calculated has impact on potential distribution models. *Methods Ecol. Evol.* **11**(12), 1559–1570 (2020).
4. Nix, H. A. A biogeographic analysis of Australian elapid snakes. *Atlas Eelapid Snakes Aust.* **7**, 4–15 (1986).
5. Robert, et al. Very high resolution interpolated climate surfaces for global land areas. *Int. J. Climatol.* **25**(15), 1965–1978 (2005).
6. Noce, S., Caporaso, L. & Santini, M. A new global dataset of bioclimatic indicators. *Sci. Data* **7**(1), 398 (2020).
7. Hijmans, R. J. et al. Very high resolution interpolated climate surfaces for global land areas. *Int. J. Climatol.: J. R. Meteorol. Soc.* **25**(15), 1965–1978 (2005).
8. Xu, T. & Hutchinson, M. ANUCLIM version 6.1 user guide 90 (Fenner School of Environment and Society, Fenner School of Environment and Society, 2011).
9. Kriticos, D. J., Jarošík, V. & Ota, N. Extending the suite of bioclim variables: a proposed registry system and case study using principal components analysis. *Methods Ecol. Evol.* **5**(9), 956–960 (2014).
10. Fick, S. E. & Hijmans, R. J. WorldClim 2: new 1km spatial resolution climate surfaces for global land areas. *Int. J. Climatol.* **37**(12), 4302–4315 (2017).
11. Brun, P. et al. Global climate-related predictors at kilometre resolution for the past and future. *Earth Syst. Sci. Data Discuss.* **2022**, 1–44 (2022).
12. Vega, G. C., Perttierra, L. R. & Ángel, O.-T.M. Erratum: MERRAclim, a high-resolution global dataset of remotely sensed bioclimatic variables for ecological modelling. *Sci. Data* **5**, 180070 (2018).
13. Otbogbayar, M. et al. Estimation of bioclimatic variables of Mongolia derived from remote sensing data. *Front. Earth Sci.* <https://doi.org/10.1007/s11707-020-0862-9> (2022).
14. Alford, D. et al. *Monitoring of glaciers, climate, and runoff in the Hindu Kush-Himalaya Mountains* (World Bank, 2012).
15. Cheval, S. et al. Identifying climate change hotspots relevant for ecosystems in Romania. *Clim. Res.* **80**(3), 165–173 (2020).
16. Liang, Q. et al. The eastern limit of 'Kunlun–Pamir–Karakoram Anomaly' reflected by changes in glacier area and surface elevation. *J. Glaciol.* **68**(272), 1167–1176 (2022).
17. Smith, T. & Bookhagen, B. Changes in seasonal snow water equivalent distribution in High Mountain Asia (1987 to 2009). *Sci. Adv.* **4**(1), e1701550 (2018).
18. Zhang, Z. et al. Glacier changes since the early 1960s, eastern Pamir, China. *J. Mt. Sci.* **13**, 276–291 (2016).
19. Wang, Y. et al. Glacier anomaly over the western Kunlun Mountains, Northwestern Tibetan Plateau, since the 1970s. *J. Glaciol.* **64**(246), 624–636 (2018).
20. Wen, T., Guo, Y., Dong, S., Dong, Y. & Lai, X., Assessment of CRU, ERA5, CMFD grid precipitation data for the Tibetan Plateau from 1979 to 2017 Arid Zone Research **39**(3), 684–697 (2021).
21. Long, R. Y. et al. An overview of temperature variations on the Qinghai-Tibetan plateau in the recent hundred years using UK CRU high resolution grid data. *J. Lanzhou Univ. (Nat. Sci.)* **48**(6), 63–68 (2012).
22. Mölg, N. et al. A consistent glacier inventory for Karakoram and Pamir derived from Landsat data: Distribution of debris cover and mapping challenges. *Earth Syst. Sci. Data* **10**(4), 1807–1827 (2018).
23. Forsythe, N. et al. Karakoram temperature and glacial melt driven by regional atmospheric circulation variability. *Nat. Clim. Chang.* **7**(9), 664–670 (2017).
24. Du, W., Jia, P. & Du, G. Current biogeographical roles of the Kunlun mountains. *Ecol. Evol.* **12**(1), e8493 (2022).
25. Chen, C. & Li, G. Temporal and spatial variation of grassland NDVI in Kunlun Mountains, Altun Mountains and Its responses to temperature and precipitation from 1981 through 2020. *Chin. J. Grassl.* **45**, 13–25 (2023).
26. Ru, H. et al. Impact of traffic noise on Tibetan antelopes: A preliminary experiment on the Qinghai-Tibet Highway in China. *Appl. Ecol. Environ. Res.* **16**(3), 2923–2932 (2018).
27. Xu, A. et al. Status and conservation of the snow leopard *Panthera uncia* in the Gouli Region, Kunlun Mountains. *China. Oryx* **42**(3), 460–463 (2008).
28. Yu, Y. et al. Geographical distribution and vicissitude of argali, *Ovis ammon*, in China. *Biodivers. Sci.* **16**(2), 197 (2008).
29. Wang, D. & Wang, A. Applicability assessment of GPCC and CRU precipitation products in China during 1901 to 2013. *Clim. Environ. Res.* **22**(4), 446–462 (2017).

30. Wang, S. et al. Drought evolution characteristics of the Qinghai-Tibet Plateau over the last 100 years based on SPEI. *Nat. Hazards Earth Syst. Sci. Discuss.* **2021**, 1–20 (2021).
31. Wei, Y. et al. Dual influence of climate change and anthropogenic activities on the spatiotemporal vegetation dynamics over the Qinghai-Tibetan plateau from 1981 to 2015. *Earth's Fut.* **10**(5), e2021EF002566 (2022).
32. Shi, H., Li, T. & Wei, J. Evaluation of the gridded CRU TS precipitation dataset with the point raingauge records over the Three-river headwaters Region. *J. Hydrol.* **548**, 322–332 (2017).
33. Theil, H. A rank-invariant method of linear and polynomial regression analysis. *Nederl. Akad. Wetensch. Proc.* **12**(2), 345–381 (1992).
34. Sen, P. K. Estimates of the regression coefficient based on Kendall's Tau. *J. Am. Stat. Assoc.* **63**(324), 1379–1389 (1968).
35. Zuo, D. et al. Time-lag effects of climatic change and drought on vegetation dynamics in an alpine river basin of the Tibet Plateau, China. *J. Hydrol.* **600**, 126532 (2021).
36. Björnsson, H. & Venegas, S. A manual for EOF and SVD analyses of climatic data. *CCGCR Rep.* **97**(1), 112–134 (1997).
37. Wu, Q. et al. Spatiotemporal variations of water conservation function based on EOF analysis at multi time scales under different ecosystems of Heihe River Basin. *J. Environ. Manage.* **325**, 116532 (2023).
38. Xu, X. et al. The spatiotemporal patterns of the upper-tropospheric water vapor over the Tibetan plateau in summer based on EOF analysis. *J. Clim.* **35**(15), 5033–5051 (2022).
39. Grinsted, A., Moore, J. C. & Jevrejeva, S. Application of the cross wavelet transform and wavelet coherence to geophysical time series. *Nonlinear Process. Geophys.* **11**(5/6), 561–566 (2004).
40. Walsh, C. & Patterson, R. Attribution of observed periodicity in extreme weather events in eastern North America. *Earth Space Sci.* **9**(7), e2022EA002359 (2022).
41. Torrence, C. & Compo, G. P. A practical guide to wavelet analysis. *Bull. Am. Meteor. Soc.* **79**(1), 61–78 (1998).
42. North, G. R. et al. Sampling errors in the estimation of empirical orthogonal functions. *Mon. Weather Rev.* **110**(7), 699–706 (1982).
43. Knight, J. Scientists' warning of the impacts of climate change on mountains. *PeerJ* **10**, e14253 (2022).
44. Rangwala, I. & Miller, J. R. Climate change in mountains: A review of elevation-dependent warming and its possible causes. *Clim. Change* **114**(3–4), 527–547 (2012).
45. Li, Y. & Chen, Y. The continuing shrinkage of snow cover in High Mountain Asia over the last 4 decades. in *EGU General Assembly Conference Abstracts* (2023).
46. Shen, M. et al. Plant phenology changes and drivers on the Qinghai-Tibetan Plateau. *Nat. Rev. Earth Environ.* **3**(10), 633–651 (2022).
47. Yu, Y. et al. Integrated warm-wet trends over the Tibetan Plateau in recent decades. *J. Hydrol.* **639**, 131599 (2024).
48. Duan, A. & Wu, G. Change of cloud amount and the climate warming on the Tibetan Plateau. *Geophys. Res. Lett.* <https://doi.org/10.1029/2006GL027946> (2006).
49. Zhang, H. & Gao, Y. Projected changes in precipitation recycling over the Tibetan Plateau based on a global and regional climate model. *J. Hydrometeorol.* **22**(10), 2633–2644 (2021).
50. Kang, S. et al. Review of climate and cryospheric change in the Tibetan Plateau. *Environ. Res. Lett.* **5**(1), 015101 (2010).
51. Li, C. et al. Variation characteristics of temperature and precipitation over the southeast Xizang since 1960. *Plateau Meteorol.* **42**(02), 344–358 (2023).
52. Pei, Y. et al. Increasing landslide activity in the Taxkorgan River Basin (eastern Pamirs Plateau, China) driven by climate change. *Catena: Interdiscip. J. Soil Sci. Hydrol.-Geomorphol. Focus. Geoccol. Landsc. Evolut.* <https://doi.org/10.1016/j.catena.2023.106911> (2023).
53. Li, G. et al. Analysis of the spatial distribution of precipitation and topography with GPM data in the Tibetan Plateau. *Atmos. Res.* **247**, 105259 (2021).
54. Boos, W. R. & Kuang, Z. Dominant control of the South Asian monsoon by orographic insulation versus plateau heating. *Nature* **463**(7278), 218–222 (2010).
55. Lambrecht, A. et al. High altitude accumulation and preserved climate information in the western Pamir, observations from the Fedchenko Glacier accumulation basin. *J. Glaciol.* **66**(256), 219–230 (2019).
56. Aichner, B. et al. Hydroclimate in the Pamirs was driven by changes in precipitation-evaporation seasonality since the last glacial period. *Geophys. Res. Lett.* **46**(23), 13972–13983 (2019).
57. Antonelli, A. et al. Geological and climatic influences on mountain biodiversity. *Nat. Geosci.* **11**(10), 718–725 (2018).
58. Huang, X. et al. Precipitation dominates the distribution of species richness on the Kunlun–Pamir Plateau. *Rem. Sens.* **14**(24), 6187 (2022).
59. Li, M.-L. et al. Assessment of habitat suitability of Ovis ammon polii based on MaxEnt modeling in Taxkorgan wildlife nature reserve. *Chin. J. Ecol.* **38**(2), 594 (2019).
60. Root, T. L. et al. Fingerprints of global warming on wild animals and plants. *Nature* **421**(6918), 57–60 (2003).
61. Wu, J. Detecting and attributing the effect of climate change on the changes in the distribution of Qinghai-Tibet plateau large mammal species over the past 50 years. *Mammal Res.* **60**, 353–364 (2015).
62. Chinanews.com. Wild animals frequently appear beneath the Kunlun Mountains (2022). <https://baijiahao.baidu.com/s?id=1721556336540007322&wfr=spider&for=pc>. Accessed 10 Jan 2022.
63. Yimingjiang, J. Z. How many rare wild animals and plants do you know in the Pamir Plateau of Xinjiang (2022). <https://baijiahao.baidu.com/s?id=1748650548613176611&wfr=spider&for=pc>. Accessed 05 Nov 2022.
64. Stein, A., Gerstner, K. & Kreft, H. Environmental heterogeneity as a universal driver of species richness across taxa, biomes and spatial scales. *Ecol. Lett.* **17**(7), 866–880 (2014).
65. Pianka, E. R. Latitudinal gradients in species diversity: a review of concepts. *Am. Nat.* **100**(910), 33–46 (1966).
66. Walther, G. R. et al. Ecological responses to recent climate change. *Nature* **416**(6879), 389–395 (2002).
67. Jian, N. An introduction to bioclimatic factors in global change research. *Quat. Sci.* **37**(3), 431–441 (2017).

Acknowledgements

This research was jointly supported by the Key R&D Program of Xinjiang Uygur Autonomous Region (Grant No. 2022B03021), the Tianshan Talent Training Program of Xinjiang Uygur Autonomous region (Grant No. 2022TSYCLJ0011), Transformation of Scientific and Technological Achievements from the Qinghai Province (Grant No. 2020-SF-145), the 2020 Qinghai Kunlun talents -Leading scientists project (Grant No. 2020-LCJ-02), and Key program of International Cooperation, Bureau of International Cooperation, Chinese Academy of Sciences (Grant No. 131551KYSB20210030).

Author contributions

X.H. Conceptualization, Data analysis, Visualization, Writing—original draft. A.B. Supervision, Writing—review and editing, Funding acquisition. Y.W. Methodology, Writing—review and editing. G.Z: Visualization, Writing—review and editing. Y.Y. Supervision, Methodology. J.B. Data collection, Visualization; T.L. Methodology, Software. T.Y.; T.W.; I. Z.; L.J.; V.N.; P. M. and T.V. Writing—review & editing.

Declarations

Competing interests

The authors declare no competing interests.

Additional information

Correspondence and requests for materials should be addressed to A.B.

Reprints and permissions information is available at www.nature.com/reprints.

Publisher's note Springer Nature remains neutral with regard to jurisdictional claims in published maps and institutional affiliations.

Open Access This article is licensed under a Creative Commons Attribution-NonCommercial-NoDerivatives 4.0 International License, which permits any non-commercial use, sharing, distribution and reproduction in any medium or format, as long as you give appropriate credit to the original author(s) and the source, provide a link to the Creative Commons licence, and indicate if you modified the licensed material. You do not have permission under this licence to share adapted material derived from this article or parts of it. The images or other third party material in this article are included in the article's Creative Commons licence, unless indicated otherwise in a credit line to the material. If material is not included in the article's Creative Commons licence and your intended use is not permitted by statutory regulation or exceeds the permitted use, you will need to obtain permission directly from the copyright holder. To view a copy of this licence, visit <http://creativecommons.org/licenses/by-nc-nd/4.0/>.

© The Author(s) 2025